# Chapter 22
# Theory and Computation of Nonlinear Damage Accumulation for Lifetime Prediction

Anton Matzenmiller & Ulrich Kroll

**Abstract** Nonlinear damage accumulation is modelled for the lifetime prediction in order to capture the loading sequence effect, which is the influence of the chronological order of the loading values on the lifetime. The prediction results from the solution of the damage evolution equation, which is defined according to the theory of continuum damage mechanics and applied together with a cohesive zone model for structural adhesive joints. The damage model consists of a creep and fatigue damage part, both taking into account the influence of the mean stress and the load multiaxiality on the predicted time to rupture. The analytical investigation of the model shows the meaning of the model parameters and propose their identification by means of tests with static and constant amplitude loading. In order to capture the loading sequence effect by nonlinear damage accumulation, the fatigue damage part is enhanced with a factor, which influences the predicted lifetime due to variable amplitude loading in the case of pure fatigue damage, while the prediction for constant amplitude loading is unaffected. The influences of the enhancement on the predicted lifetime and the damage evolution are discussed. The comparison of lifetimes with numerical predictions proves the validity of the proposed approach.

**Keywords:** Damage mechanics · Lifetime prediction · Adhesive joints

## 22.1 Introduction

Components in engineering applications suffer sustained mechanical service loading. In the particular case, where two constant values exist for each the local maxima and minima, which e. g. is the case for the harmonic, sawtooth wave or triangle

Anton Matzenmiller · Ulrich Kroll
Institute of Mechanics, Department of Mechanical Engineering, University of Kassel, Mönchebergstraße 7, 34125 Kassel, Germany,
e-mail: amat@uni-kassel.de, ulrich.kroll@uni-kassel.de



B. E. Abali et al. (eds.), *New Achievements in Continuum Mechanics and Thermodynamics*, Advanced Structured Materials 108,
https://doi.org/10.1007/978-3-030-13307-8_22

wave function, service loading is called constant amplitude (CA) loading, otherwise variable amplitude (VA) loading. Fatigue damage is contributed due to each loading cycle, which may be defined by the load reversals of two neighbouring local maxima or minima of the service loading and the corresponding values in between. In high cycle fatigue (HCF), fatigue damage is accumulated over a large number of loading cycles – usually more than several tens of thousands up to millions – and causes the gradual degradation of the integrity (load bearing capacity) at a material point. After a certain time, the material lifetime, the complete integrity of the material point is lost and a local crack initiates. The loading continues and the crack grows, while other cracks may initiate and grow at different material points. As a consequence of this process of degradation, after some time, the structural lifetime, there remains no load bearing capacity of the structure, which leads to fatal failure of the component. Therefore, the operation time of the component must not exceed its lifetime, which has to be ensured by lifetime prediction.

The lifetime prediction for components and structures is generally performed by use of technical codes and guidelines, e. g. Normenausschuss Bauwesen (NABau) im DIN (2010, 2011); Rennert et al (2012) for steel and aluminium components. These guidelines propose empirical methods, which are highly adapted to particular applications and make use of a variety of simplifying assumptions for the process of fatigue. Most of the assumptions apply superposition, which leads to linearity. Therefore, nonlinear phenomena are not captured, although they may have a great influence on the material and the structural lifetime. One of these nonlinear phenomena is the loading sequence effect, which is the influence of the chronological order of the loading values on the lifetime. The sequence effect is modelled with so called nonlinear damage accumulation, for which the damage increments cannot be easily superimposed, which is usually the case in common procedures for lifetime prediction. Nevertheless, several lifetime prediction methods introduce influencing factors for the consideration of nonlinear phenomena for the particular component, material and application, e. g. influencing factors for temperature, surface condition, loading sequence, mean stress, frequency, multiaxiality etc. Such methods cannot be easily transferred to different materials and structures and are not able to be applied in general. As a consequence, different lifetime prediction methods have been proposed for various materials, components and applications. Furthermore, because of this lack of generality, there exist no commonly accepted lifetime prediction methods for a number of joining techniques such as adhesive bonding.

Continuum damage mechanics (CDM) strives to overcome this shortcoming. In contrast to conventional methods, the lifetime prediction for the structure is an outcome of the lifetime prediction for each material point and the consideration of the whole loading process. The representation of all material phenomena results from the definition of the constitutive equations for the stress and the internal variables in the framework of continuum mechanics. Thereby, one internal variable represents material damage, which evolution equation is adapted to the description of the fatigue process in order to predict the material lifetime.

The lifetime prediction with CDM started with the approach in Kachanov (1958) for the prediction of the creep rupture time of brittle materials in the uniaxial case

by means of the definition of the so called continuity, which stands for structural integrity. In Lemaitre and Chaboche (1975), first, damage is defined as the contrary variable to the continuity. Second, the approach in Kachanov (1958) is extended for nonlinear creep damage accumulation and, third, a creep-fatigue damage model is proposed, for which the formalism of the creep damage approach in Kachanov (1958) is transferred to fatigue damage. The creep-fatigue damage model in Lemaitre and Chaboche (1975) is a differential equation in terms of differential damage, time and loading cycles. The model extension for multiaxial loading and plastic damage is proposed in Lemaitre (1979), where the inclusion of the damage theory into thermodynamics of irreversible processes is also addressed. The predicted creep-fatigue damage interaction of the proposed theory is presented in Lemaitre and Plumtree (1979); Cailletaud and Levaillant (1984) and Cailletaud et al (1984), where two-level loadings with pure creep and pure fatigue levels are considered. In Chaboche (1981), the theory of CDM and its application for lifetime prediction are reviewed, accompanied by further studies of creep-fatigue damage interaction and one of the first approaches for the application of CDM for anisotropic damage, which has been also initially investigated in Murakami and Ohno (1981). In Chaboche (1978); Lemaitre (1984), an enhancement of the model in Lemaitre and Chaboche (1975) for the consideration of nonproportional loading is presented. The developed methods and approaches of CDM for lifetime prediction are reviewed again in Lemaitre (1984); Chaboche (1987); Krajcinovic and Lemaitre (1987); Chaboche (1988a,b). In Chaboche and Lesne (1988), the main features of the approach in Lemaitre and Chaboche (1975) are reviewed and discussed. The lifetime prediction with CDM has been further developed in Paas et al (1993) and applied in Lemaitre and Doghri (1994). All the results mentioned before are part of the monographs Lemaitre and Chaboche (1990); Lemaitre (1996); Lemaitre and Desmorat (2005). In Lemaitre and Desmorat (2005), the extension of the proposed approaches with criterions suitable for fatigue damage evolution due to nonproportional loading is mentioned. A short review of the theory and a discussion of improvements for future investigations are presented in Chaboche (2003). In Chaboche (2011), several models for nonlinear damage accumulation are discussed, including the model in Lemaitre and Chaboche (1975) and Chaboche and Lesne (1988).

In CDM, the solution of the damage differential equation results in the predicted number of cycles until rupture for a given stress level. This result is called stress-number (S-N) model, which e. g. takes the form of the Basquin equation (Basquin, 1910) and represents the influence of the amplitude of mechanical CA loading on the lifetime. Other influences of CA loading are related to mean stress, frequency, difference of tension and compression as well as multiaxiality. As in the case of the influence of the amplitude, all these influences are considered by the solution of the damage differential equation. Even the influence of nonproportional (out of phase) loading can be taken into account, which may result from different phases of the stress components. For VA loading, it is well known that also the load-level sequence has an effect on the lifetime (Lemaitre and Chaboche, 1990). The modelling of this effect by nonlinear damage accumulation is of great importance for the warranty of fatigue durability due to lifetime prediction, since linear damage accu-

mulation generally leads to a significant overestimation of the lifetime for complex VA loading cases, based on load spectra and standardised loadings from measurements during service (Chaboche, 2011, p. 50). This observation is also made for adhesives, see Erpolat et al (2004). Hence, the loading sequence effect must be considered in order to prevent the overestimation of the lifetime of adhesively bonded components and possible disastrous consequences.

In this contribution, a creep-fatigue damage model is presented and its consideration of the loading sequence effect by nonlinear damage accumulation is explained in detail. Although the model at hand is applied through a cohesive zone model for the lifetime prediction of adhesively bonded joints, the general characteristics for the consideration of the loading sequence effect can be directly transferred and applied for the lifetime prediction of various materials.

## 22.2 Modelling of Damage Growth

The theory of CDM is transferred to the cohesive zone model, relating the separation $\boldsymbol{\Delta}$ via the constitutive equation to traction $\mathbf{t} = \left[t_\mathrm{t}\ t_\mathrm{b}\ t_\mathrm{n}\right]^\mathsf{T}$, which consists of the tangential $t_\mathrm{t}$, binormal $t_\mathrm{b}$ and normal stress component $t_\mathrm{n}$ and is calculated according to effective stress concept (Rabotnov, 1963, 1969) for the multiaxial case (Murakami and Ohno, 1981; Lemaitre and Chaboche, 1990):

$$\mathbf{t} = (1 - D)\tilde{\mathbf{t}}\ ,\ D \in [0, 1]\ . \tag{22.1}$$

The effective traction $\tilde{\mathbf{t}} = \tilde{\mathbf{t}}(\boldsymbol{\Delta})$ represents the material behaviour without consideration of damage $D$. Every damage free model can be used for the effective traction $\tilde{\mathbf{t}}$, e. g. constitutive equations for a (visco-)elastic-(visco-)plastic cohesive model. The damage free state is characterised by $D = 0$. Mechanical loading causes initiation and growth of voids and, thus, increase of damage, which results in $D > 0$. If mechanical loading is further applied, then this process continues until local rupture at $D = 1$. For this damage evolution, a differential equation must be defined, which has to be suitable for the particular case of application. The additive split of the damage increment $\mathrm{d}D$ is proposed in Lemaitre and Chaboche (1975) for lifetime prediction: damage consists of the creep $\mathrm{d}D_\mathrm{c}$ and fatigue damage part $\mathrm{d}D_\mathrm{f}$, both caused by sustained loading:

$$\mathrm{d}D = \mathrm{d}D_\mathrm{c} + \mathrm{d}D_\mathrm{f}\ . \tag{22.2}$$

Based on this idea, Eq. (22.2) is reformulated in Matzenmiller and Kurnatowski (2012); Kroll and Matzenmiller (2017) in order to define a differential equation in time according to the general framework of continuum mechanics with internal variables (Truesdell and Toupin, 1960; Coleman and Gurtin, 1967):

$$\dot{D} = \dot{D}_\mathrm{c} + \dot{D}_\mathrm{f}\ . \tag{22.3}$$

For the lifetime prediction in the case of long-term sustained static and cyclic loading, the creep $\dot{D}_\mathrm{c}$ and fatigue damage evolution $\dot{D}_\mathrm{f}$ must be specified. In view of the additive split of creep and fatigue damage in Eq. (22.3), creep damage should primarily evolve due to creep loading while fatigue damage should mainly evolve due to loading cycles.

### *22.2.1 Creep Damage Evolution*

For the creep damage evolution $\dot{D}_\mathrm{c}$ in Eq. (22.3), the following model is proposed in Matzenmiller and Kurnatowski (2012) and based on the uniaxial version in Kachanov (1958):

$$\dot{D}_\mathrm{c} = \frac{1}{c_0}\left(\frac{\langle \sigma_\mathrm{eqc} - \sigma_\mathrm{dc}\rangle}{\sigma_\mathrm{ref}(1-D)}\right)^n \quad , \quad c_0 = 1\ \mathrm{s}\ . \tag{22.4}$$

Creep damage evolves due to the following equivalent stress, which depends on the tractions in Eq. (22.1) and reads

$$\sigma_\mathrm{eqc} = \sqrt{\langle b_{1\mathrm{c}} t_\mathrm{n}^2 + b_{2\mathrm{c}} t_\mathrm{n} + t_\mathrm{t}^2 + t_\mathrm{b}^2\rangle}\ , \tag{22.5}$$

where positive tractions $t_\mathrm{i} > 0$, $i = \mathrm{t}, \mathrm{b}, \mathrm{n}$ are assumed for simplicity. Hence, alternating stress and pressure are not considered in this contribution but are addressed in Kroll and Matzenmiller (2017); Kroll (2018). The parameters $b_{1\mathrm{c}}$ and $b_{2\mathrm{c}}$ in Eq. (22.5) take into account the multiaxiality of the loading (Kroll and Matzenmiller, 2017; Kroll, 2018). The constant $c_0$ in Eq. (22.4) is introduced for consistent units. The Macaulay operator $\langle x\rangle = (x + |x|)/2$ in Eq. (22.4) results in no creep damage evolution, if the loading is below the creep limit $\sigma_\mathrm{dc}$. The meaning of the two remaining creep damage model parameters $n$ and $\sigma_\mathrm{ref}$ is demonstrated by means of creep loading, for which the tractions in Eq. (22.1) are constant: $t_\mathrm{i} = \mathrm{const.}$, $i = \mathrm{t}, \mathrm{b}, \mathrm{n}$. If creep loading results in pure creep damage in Eq. (22.3), i. e. $\dot{D}_\mathrm{f} = 0$, $D = D_\mathrm{c}$, then Eq. (22.4) yields

$$\dot{D}_\mathrm{c} = \frac{1}{c_0}\left(\frac{\langle \sigma_\mathrm{eqc} - \sigma_\mathrm{dc}\rangle}{\sigma_\mathrm{ref}(1-D_\mathrm{c})}\right)^n \ . \tag{22.6}$$

If separation and integration are applicable, then the characteristics of the damage differential equation for lifetime prediction arise from three solutions, which are obtained by use of different limits.

For the first solution of Eq. (22.6), separation and integration of the damage equation (22.6) from zero damage $D = 0$ at time $t = 0$ until total failure $D = 1$ at rupture time $t_\mathrm{R}$ for creep loading $\sigma_\mathrm{eqc} = \mathrm{const.} > \sigma_\mathrm{dc}$ results in the following expression, cf. Kachanov (1958):

$$\int_0^1 (1-D_\mathrm{c})^n \mathrm{d}D_\mathrm{c} = \int_0^{t_\mathrm{R}} \frac{1}{c_0}\left(\frac{\sigma_\mathrm{eqc}-\sigma_\mathrm{dc}}{\sigma_\mathrm{ref}}\right)^n \mathrm{d}t \Rightarrow t_\mathrm{R} = \frac{c_0}{n+1}\left(\frac{\sigma_\mathrm{ref}}{\sigma_\mathrm{eqc}-\sigma_\mathrm{dc}}\right)^n . \tag{22.7}$$

Application of the logarithm and rearrangement of terms yields the double logarithmic straight line

$$\ln\left(\sigma_\mathrm{eqc}-\sigma_\mathrm{dc}\right) = -\frac{1}{n}\ln\frac{t_\mathrm{R}}{c_0} + \ln\frac{\sigma_\mathrm{ref}}{(n+1)^{\frac{1}{n}}} . \tag{22.8}$$

The meaning of the creep damage parameters $n$ and $\sigma_\mathrm{ref}$ becomes apparent in Eq. (22.8), which is illustrated in Fig. 22.1(a): Parameter $n$ determines the slope of the double logarithmic straight line and $\sigma_\mathrm{ref}$ stands for the ordinate value for fixed $n$.

The second solution of Eq. (22.6) is performed for a virgin material with $D = 0$ at $t = 0$ until damage $D$ at time $t$ for creep loading $\sigma_\mathrm{eqc} = \mathrm{const.}$, $\sigma_\mathrm{eqc} > \sigma_\mathrm{dc}$, see Lemaitre and Chaboche (1975):

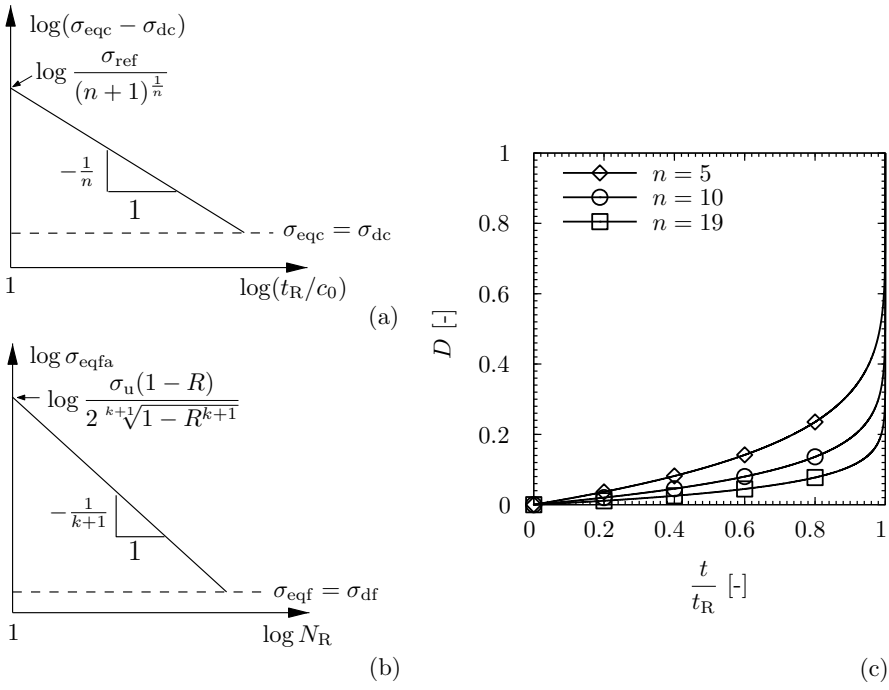


**Fig. 22.1** Influence of parameters: (a) influence of creep damage parameters on predicted time to rupture; (b) influence of fatigue damage parameters on predicted number of cycles to rupture; (c) influence of parameter $n$ on damage evolution over normalised time according to Eq. (22.9)

$$\int_0^D (1-D_\mathrm{c})^n \,\mathrm{d}D_\mathrm{c} = \int_0^t \frac{1}{c_0}\left(\frac{\sigma_\mathrm{eqc}-\sigma_\mathrm{dc}}{\sigma_\mathrm{ref}}\right)^n \mathrm{d}\tilde{t} \Rightarrow D = 1-\left(1-\frac{t}{t_\mathrm{R}}\right)^{\frac{1}{n+1}} . \tag{22.9}$$

Equation (22.7) has been used for the substitution of rupture time $t_\mathrm{R}$ in Eq. (22.9), which is illustrated in Fig. 22.1(c): The parameter $n$ influences the evolution of damage $D$ over normalised time $t/t_\mathrm{R}$ between the fixed start and end point at $D = 0$ and $D = 1$. In contrast, the parameters $\sigma_\mathrm{dc}$ and $\sigma_\mathrm{ref}$ do not influence the curve at all.

The third solution of Eq. (22.6) is obtained by separation and integration from damage $D_{i-1}$ at time $t_{i-1}$ to new damage state $D_i$ due to loading $\sigma_{\mathrm{eqc},i} = \mathrm{const.}$, acting over time $\Delta t_i$ (Lemaitre and Plumtree, 1979):

$$\int_{D_{i-1}}^{D_i} (1-D_\mathrm{c})^n \,\mathrm{d}D_\mathrm{c} = \int_{t_{i-1}}^{t_{i-1}+\Delta t_i} \frac{1}{c_0}\left(\frac{\sigma_{\mathrm{eqc},i}-\sigma_\mathrm{dc}}{\sigma_\mathrm{ref}}\right)^n \mathrm{d}t \,, \tag{22.10}$$

$$D_i = 1-\left((1-D_{i-1})^{n+1} - \frac{\Delta t_i}{t_{\mathrm{R}i}}\right)^{\frac{1}{n+1}} . \tag{22.11}$$

In Eq. (22.11), $t_{\mathrm{R}i}$ denotes the time to rupture, if creep loading with $\sigma_{\mathrm{eqc},i}$ is applied from the undamaged state until total failure, i. e. Eq. (22.7) with $t_{\mathrm{R}i}$ instead of $t_\mathrm{R}$ and $\sigma_{\mathrm{eqc},i}$ instead of $\sigma_\mathrm{eqc}$. Eq. (22.11) represents the actual damage value $D_i$ after the so called load level or load block $i = 1, ..., K$ of a $K$-level or $K$-block creep loading sequence in form of a recurrence relation.

### *22.2.2 Fatigue Damage Evolution*

The following model for fatigue damage evolution $\dot{D}_\mathrm{f}$ is based on the approach in terms of loading cycles in Lemaitre (1979) and proposed in Matzenmiller and Kurnatowski (2012) for the approach in Eq. (22.3):

$$\dot{D}_\mathrm{f} = \left(\frac{\langle\sigma_\mathrm{eqf}-\sigma_\mathrm{df}\rangle}{(\sigma_\mathrm{u}-\sigma_\mathrm{df})(1-D)}\right)^k \frac{\langle\dot{\sigma}_\mathrm{eqf}\rangle}{\sigma_\mathrm{u}-\sigma_\mathrm{df}} . \tag{22.12}$$

The equivalent stress depends on the tractions in Eq. (22.1) and is defined as

$$\sigma_\mathrm{eqf} = \sqrt{\langle b_{1\mathrm{f}} t_\mathrm{n}^2 + b_{2\mathrm{f}} t_\mathrm{n} + t_\mathrm{t}^2 + t_\mathrm{b}^2\rangle} \,, \tag{22.13}$$

whereby positive tractions $t_\mathrm{i} > 0$, $i = \mathrm{t,b,n}$ are considered for simplicity. As mentioned before in Sect. 22.2.1, alternating stress and pressure are not considered here but are addressed in Kroll and Matzenmiller (2017); Kroll (2018). Note that $\dot{D}_\mathrm{f} = 0$, if $\dot{\sigma}_\mathrm{eqf} \leq 0$, which includes creep loading $t_\mathrm{i} = \mathrm{const.}$, $i = \mathrm{t,b,n}$, yielding

pure creep damage evolution, which has been assumed for Eq. (22.6). The parameters $b_{1\mathrm{f}}$ and $b_{2\mathrm{f}}$ in Eq. (22.13) take the multiaxiality of the loading into consideration (Kroll and Matzenmiller, 2017; Kroll, 2018). Obviously, the parameter $\sigma_{\mathrm{df}}$ in Eq. (22.12) represents the fatigue limit. The meaning of the two remaining fatigue damage parameters $k$ and $\sigma_{\mathrm{u}}$ becomes apparent, if pure fatigue damage is assumed, i. e. $\dot{D}_{\mathrm{c}} = 0$, $D = D_{\mathrm{f}}$. Then, Eqs. (22.3) and (22.12) are represented by

$$(1 - D_{\mathrm{f}})^k \mathrm{d}D_{\mathrm{f}} = \frac{1}{(\sigma_{\mathrm{u}} - \sigma_{\mathrm{df}})^{k+1}} \left\langle \sigma_{\mathrm{eqf}} - \sigma_{\mathrm{df}} \right\rangle^k \left\langle \mathrm{d}\sigma_{\mathrm{eqf}} \right\rangle , \tag{22.14}$$

where separation of variables has been applied. As in the previous Sect. 22.2.1, the characteristics of the damage equation (22.14) result from three solutions in form of integrations with different limits.

The first solution results from the integration of damage free material with $D = 0$ until rupture at $D = 1$ due to the periodic loading $\sigma_{\mathrm{eqf}}(t) = \sigma_{\mathrm{eqf}}(t + T)$ with smallest period $T$ as well as local and global minimum $\sigma_{\mathrm{eqfmin}} = \min \sigma_{\mathrm{eqf}}$ and maximum $\sigma_{\mathrm{eqfmax}} = \max \sigma_{\mathrm{eqf}}$. An example of such a loading is the harmonic function

$$\sigma_{\mathrm{eqf}} = \sigma_{\mathrm{eqfm}} + \sigma_{\mathrm{eqfa}} \sin(2\pi f t) \tag{22.15}$$

with mean stress $\sigma_{\mathrm{eqfm}}$, stress amplitude $\sigma_{\mathrm{eqfa}}$ and frequency $f = 1/T$. Consequently, Eq. (22.14) can be integrated over period $T$, which corresponds to the integration over a stress cycle, consisting of the stress values within the periodic time. The stress cycle results in a damage increment $\Delta D$, thus, Eq. (22.14) becomes

$$\int_{D}^{D+\Delta D} (1 - D_{\mathrm{f}})^k \mathrm{d}D_{\mathrm{f}} = \frac{1}{(\sigma_{\mathrm{u}} - \sigma_{\mathrm{df}})^{k+1}} \oint_{\sigma_{\mathrm{eqf}}} \left\langle \sigma_{\mathrm{eqf}} - \sigma_{\mathrm{df}} \right\rangle^k \left\langle \mathrm{d}\sigma_{\mathrm{eqf}} \right\rangle . \tag{22.16}$$

The Macaulay operator in Eq. (22.16) results in $\langle \mathrm{d}\sigma_{\mathrm{eqf}} \rangle = 0$, if $\sigma_{\mathrm{eqf}}$ decreases, which is the case for the integration from $\sigma_{\mathrm{eqfmax}}$ to $\sigma_{\mathrm{eqfmin}}$. Additionally, the simplifying assumption $\sigma_{\mathrm{eqf}} > \sigma_{\mathrm{df}}$ is applied in the following. Furthermore, the number of periodic load repetitions $N$ is introduced, which is called cycle number and described as dimensionless time (Paas et al, 1993). Hence, Eq. (22.16) becomes

$$\int_{D}^{D+\Delta D} (1 - D_{\mathrm{f}})^k \mathrm{d}D_{\mathrm{f}} = \frac{1}{(\sigma_{\mathrm{u}} - \sigma_{\mathrm{df}})^{k+1}} \int_{N}^{N+1} \int_{\sigma_{\mathrm{eqfmin}}}^{\sigma_{\mathrm{eqfmax}}} \left( \sigma_{\mathrm{eqf}} - \sigma_{\mathrm{df}} \right)^k \mathrm{d}\sigma_{\mathrm{eqf}} \mathrm{d}\tilde{N} . \tag{22.17}$$

For simplicity and without loss of generality, it is assumed that rupture occurs immediately after a certain cycle. Then, Eq. (22.17) results in the following expression for the number of cycles to rupture $N_{\mathrm{R}}$:

$$\int_0^1 (1-D_\mathrm{f})^k \mathrm{d}D_\mathrm{f} = \frac{1}{(\sigma_\mathrm{u}-\sigma_\mathrm{df})^{k+1}} \int_0^{N_\mathrm{R}} \int_{\sigma_\mathrm{eqfmin}}^{\sigma_\mathrm{eqfmax}} (\sigma_\mathrm{eqf}-\sigma_\mathrm{df})^k \,\mathrm{d}\sigma_\mathrm{eqf}\mathrm{d}\tilde{N}, \quad (22.18)$$

$$N_\mathrm{R} = \frac{(\sigma_\mathrm{u}-\sigma_\mathrm{df})^{k+1}}{(\sigma_\mathrm{eqfmax}-\sigma_\mathrm{df})^{k+1} - (\sigma_\mathrm{eqfmin}-\sigma_\mathrm{df})^{k+1}} \,. \quad (22.19)$$

In the case of cyclic loading given by Eq. (22.15), the load ratio $R = \sigma_\mathrm{eqfmin}/\sigma_\mathrm{eqfmax}$ may be introduced. If $\sigma_\mathrm{df} = 0$, Eq. (22.19) is equivalent to the most common S-N model known as the Basquin equation (Basquin, 1910):

$$\ln \sigma_\mathrm{eqfa} = -\frac{1}{k+1} \ln N_\mathrm{R} + \ln \frac{\sigma_\mathrm{u}(1-R)}{2\sqrt[k+1]{1-R^{k+1}}} \,. \quad (22.20)$$

The influence of mean stress on the rupture time is considered by the creep damage part in Eq. (22.4) and also by the fatigue damage part in Eq. (22.12), since the stress amplitude for a given number of cycles to rupture depends on the load ratio $R$ in Eq. (22.20) for pure fatigue damage. The following solution for damage over normalised loading cycles is almost similar to Eq. (22.9): The integration from the damage free state $D = 0$ at cycle $\tilde{N} = 0$ until damage $D$ at cycle $\tilde{N} = N$ for constant amplitude loading in Eq. (22.15) with $\sigma_\mathrm{eqf} > \sigma_\mathrm{df}$ results in

$$\int_0^D (1-D_\mathrm{f})^k \mathrm{d}D_\mathrm{f} = \int_0^N \int_{\sigma_\mathrm{eqfmin}}^{\sigma_\mathrm{eqfmax}} \frac{(\sigma_\mathrm{eqf}-\sigma_\mathrm{df})^k}{(\sigma_\mathrm{u}-\sigma_\mathrm{df})^{k+1}} \mathrm{d}\sigma_\mathrm{eqf}\mathrm{d}\tilde{N} \Rightarrow D = 1 - \left(1 - \frac{N}{N_\mathrm{R}}\right)^{\frac{1}{k+1}}. \quad (22.21)$$

Equation (22.19) has been used for the substitution of the number of loading cycles until rupture $N_\mathrm{R}$. Damage in Eq. (22.21) is almost similar to the expression in Eq. (22.9). Hence, parameter $k$ has the same influence as parameter $n$, illustrated in Fig. 22.1(c).

The third solution is obtained by integration from damage $D_{i-1}$ at cycle $N_{i-1}$ to new damage state $D_i$ due to constant amplitude loading with minimum $\sigma_{\mathrm{eqfmin},i}$ and maximum $\sigma_{\mathrm{eqfmax},i}$ over $\Delta N_i$ cycles (Lemaitre and Plumtree, 1979):

$$\int_{D_{i-1}}^{D_i} (1-D_\mathrm{f})^k \mathrm{d}D_\mathrm{f} = \frac{1}{(\sigma_\mathrm{u}-\sigma_\mathrm{df})^{k+1}} \int_{N_{i-1}}^{N_{i-1}+\Delta N_i} \int_{\sigma_{\mathrm{eqfmin},i}}^{\sigma_{\mathrm{eqfmax},i}} (\sigma_\mathrm{eqf}-\sigma_\mathrm{df})^k \,\mathrm{d}\sigma_\mathrm{eqf}\mathrm{d}\tilde{N}, \quad (22.22)$$

$$D_i = 1 - \left((1-D_{i-1})^{k+1} - \frac{\Delta N_i}{N_{\mathrm{R}i}}\right)^{\frac{1}{k+1}} \,. \quad (22.23)$$

The number of cycles to rupture $N_{\mathrm{R}i}$ in Eq. (22.23) denotes the lifetime, if constant amplitude loading with minimum $\sigma_{\mathrm{eqfmin},i}$ and maximum $\sigma_{\mathrm{eqfmax},i}$ is applied from the damage free state until rupture, i. e. Eq. (22.19) with $N_{\mathrm{R}i}$ instead of $N_\mathrm{R}$, $\sigma_{\mathrm{eqfmin},i}$ instead of $\sigma_\mathrm{eqfmin}$ and $\sigma_{\mathrm{eqfmax},i}$ instead of $\sigma_\mathrm{eqfmax}$. Similar to Eq. (22.11),

which results from pure creep damage, Eq. (22.23) is also a recurrence relation for the calculation of pure fatigue damage for $K$-level constant amplitude loading.

## 22.3 Damage Accumulation

If a certain load level of a $K$-level loading is applied, then the time spent on that load level results in a corresponding damage increment. Damage accumulation is the model property, which defines, how a certain damage increment is contributed to the actual amount of damage. If the damage accumulation contains the sum of the damage increments, then the damage accumulation is called linear, otherwise nonlinear. The property of linearity refers to the commutativity of the sum, which is equal to the superposition of the damage increments regardless of their chronological appearance. Thus, a model, which exhibits linear damage accumulation, does not account for the loading sequence effect, while a model with nonlinear damage accumulation does. This is illustrated by means of the two-level creep loading until rupture in Fig. 22.2.

The loadings $\sigma_1$ and $\sigma_2$ in Fig. 22.2(a) lead to the rupture times $t_{\mathrm{R1}}$ and $t_{\mathrm{R2}}$. In the top illustration of Fig. 22.2(b), $\sigma_1$ is applied from $t = 0$ until $t = \Delta t_1 = 0.5 t_{\mathrm{R1}}$, followed by $\sigma_2$ from $t = \Delta t_1$ until rupture, which is observed after $\Delta t_2 = 0.5 t_{\mathrm{R2}}$, so $t_{\mathrm{R12}} = \Delta t_1 + \Delta t_2$. This is a High-Low (HL) creep loading sequence, since $\sigma_1 > \sigma_2$. In the case of linear damage accumulation, the same rupture time is observed, if the chronological order of the loadings is interchanged, see the Low-High (LH) creep loading scenario in the bottom illustration of Fig. 22.2(b). The loading sequence effect is not captured, since the HL and LH loading result in the same rupture time: $t_{\mathrm{R12}} = t_{\mathrm{R21}}$. This fact is represented by the Robinson rule for linear creep damage accumulation (Robinson, 1938) with $K = 2$ in the case of Fig. 22.2(b):

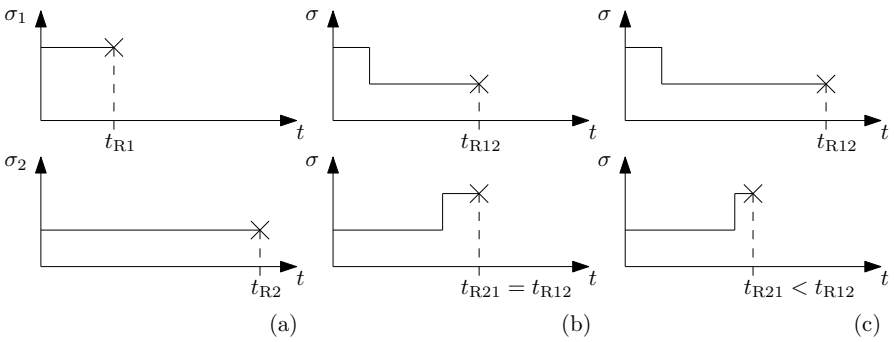


**Fig. 22.2** Illustration of damage accumulation by means of two level loading until rupture ($\times$): (a) considered loadings $\sigma_1$ and $\sigma_2$ leading to rupture times $t_{\mathrm{R1}}$ and $t_{\mathrm{R2}}$; (b) example for linear damage accumulation; (c) example for nonlinear damage accumulation

$$\sum_{i=1}^{K} \frac{\Delta t_i}{t_{\mathrm{R}i}} = 1 \ . \tag{22.24}$$

The time spent on load level $i$ is denoted with $\Delta t_i$, while $t_{\mathrm{R}i}$ is the rupture time in the case, where the loading of load level $i$ is applied as one-level loading from the undamaged material at $t = 0$ until rupture. Fig. 22.2(c) shows nonlinear damage accumulation, where the rupture times for both scenarios are not equal. A loading sequence effect is observed and Eq. (22.24) is not fulfilled anymore: The sum of creep life ratios is not always equal to one, see e.g. Pavlou (2001), where LH creep loading test data are shown, which correspond to the bottom illustration in Fig. 22.2(c).

The theory of creep damage accumulation is directly transferred to fatigue loading. Linear fatigue damage accumulation is represented by the PALMGREN–MINER rule (Palmgren, 1924; Miner, 1945), where $\Delta N_i$ denotes the number of cycles spent on load level $i$ and $N_{\mathrm{R}i}$ represents the number of cycles to rupture in the case, where the loading of load level $i$ is applied as one-level loading from $t = 0$ until rupture:

$$\sum_{i=1}^{K} \frac{\Delta N_i}{N_{\mathrm{R}i}} = 1 \ . \tag{22.25}$$

As the ROBINSON rule in Eq. (22.24), the PALMGREN–MINER rule in Eq. (22.25) also does not take the loading sequence effect into consideration.

### *22.3.1 Creep and Fatigue Damage Accumulation*

In the following, the accumulation of damage is presented due to the evolutions in the cases of pure creep and fatigue given in Eqs. (22.6) and (22.14). Damage due to creep loading over time $\Delta t_1$ is according to Eq. (22.9) and Eq. (22.11) with $i = 1$ and $D_0 = 0$

$$D_1 = 1 - \left(1 - \frac{\Delta t_1}{t_{\mathrm{R}1}}\right)^{\frac{1}{n+1}} \ . \tag{22.26}$$

Equation (22.11) with $i = 2$ is applied for the case, where a second creep loading follows and acts over time $\Delta t_2$:

$$D_2 = 1 - \left((1 - D_1)^{n+1} - \frac{\Delta t_2}{t_{\mathrm{R}2}}\right)^{\frac{1}{n+1}} \ . \tag{22.27}$$

Inserting of Eq. (22.26) into (22.27) results in

$$D_2 = 1 - \left(1 - \sum_{i=1}^{2} \frac{\Delta t_i}{t_{\mathrm{R}i}}\right)^{\frac{1}{n+1}} \ . \tag{22.28}$$

This process can be continued, which results in the amount of pure creep damage $D_j$ after load level $j$:

$$D_j = 1 - \left(1 - \sum_{i=1}^{j} \frac{\Delta t_i}{t_{\mathrm{R}i}}\right)^{\frac{1}{n+1}} . \tag{22.29}$$

Occurrence of rupture after $K$ load levels results the ROBINSON rule in Eq. (22.24):

$$D_K = 1 = 1 - \left(1 - \sum_{i=1}^{K} \frac{\Delta t_i}{t_{\mathrm{R}i}}\right)^{\frac{1}{n+1}} \Leftrightarrow \sum_{i=1}^{K} \frac{\Delta t_i}{t_{\mathrm{R}i}} = 1 . \tag{22.30}$$

Thus, the damage evolution equation (22.6) represents linear damage accumulation and cannot take the loading sequence effect into consideration.

The same result is obtained for the case of pure fatigue damage by consideration of Eq. (22.14). Damage after load level $j$ is

$$D_j = 1 - \left(1 - \sum_{i=1}^{j} \frac{\Delta N_i}{N_{\mathrm{R}i}}\right)^{\frac{1}{k+1}} , \tag{22.31}$$

where Eqs. (22.21) and (22.23) have been taken into account and a similar procedure to Eqs. (22.26) to (22.29) is applied. Equation (22.31) has the same form as Eq. (22.29). Consequently, if rupture occurs after the application of $K$ load levels, then

$$D_K = 1 = 1 - \left(1 - \sum_{i=1}^{K} \frac{\Delta N_i}{N_{\mathrm{R}i}}\right)^{\frac{1}{k+1}} \Leftrightarrow \sum_{i=1}^{K} \frac{\Delta N_i}{N_{\mathrm{R}i}} = 1 , \tag{22.32}$$

which is the PALMGREN–MINER rule, given by Eq. (22.25).

According to the results in Eqs. (22.30) and (22.32), the damage evolution equations for pure creep and pure fatigue damage exhibit linear damage accumulation. This is a result of the separability of the differential equations: All damage differential equations, which are separable, lead to linear damage accumulation (Ostergren and Krempl, 1979; Todinov, 2001). A model with nonlinear damage evolution as in Eqs. (22.9) or (22.21) does not automatically represent nonlinear damage accumulation (Chaboche and Lesne, 1988; Lemaitre and Chaboche, 1990).

### *22.3.2 Modelling of Nonlinear Damage Accumulation*

Since separability of the damage equation leads to linear damage accumulation, a model must not be separable in order to represent nonlinear damage accumulation and to account for the loading sequence effect. In the previous section, only pure creep and pure fatigue damage evolution given by Eqs. (22.6) and (22.14) have

been considered. But, the differential equation (22.3) with the approaches in Eqs. (22.4) and (22.12) is not separable for $n \neq k$ and, in this case, represents nonlinear damage accumulation through nonlinear damage interaction.

However, in practice, two circumstances lead to linear or almost linear damage accumulation of the model given by Eqs. (22.3), (22.4) and (22.12). First, the result of the parameter identification and numerical optimisation for the prediction in the case of creep and CA loading may be $n = k$, see Kroll and Matzenmiller (2017) or Cavdar et al (2018), which leads to separability and linear damage accumulation. Second, even if the identification and optimisation for other test data results in $n \neq k$, the nonlinearity of damage interaction and of the resulting damage accumulation may only weakly pronounced, see Kroll and Matzenmiller (2016). This is explained by negligible creep damage: The magnitude of the factor in (22.12) with the time derivative of the equivalent fatigue stress is of second order for usual HCF loading, e. g. Eq. (22.15) with $\sigma_{\mathrm{eqfm}} = \sigma_{\mathrm{eqfa}} = f = 10$ and pure shear $t_{\mathrm{n}} = 0$, $\sigma_{\mathrm{eqc}} = \sigma_{\mathrm{eqf}}$. In addition, if the terms with the exponent $n$ and $k$ in Eqs. (22.4) and (22.12) have the same orders of magnitude as a result of the identification, see Kroll and Matzenmiller (2015, 2016, 2017) and Kroll (2018), then creep damage evolution appears to be negligible compared to fatigue damage evolution: $\dot{D}_{\mathrm{c}} \approx 0$. But $\dot{D}_{\mathrm{c}} = 0$ is the condition to match Eqs. (22.3), (22.4), (22.12) with Eq. (22.14), which is separable and represents linear damage accumulation according to Eq. (22.32). Thus, if creep damage is negligible compared to fatigue damage for usual HCF loading, then the model Eqs. (22.3), (22.4) and (22.12) represent linear damage accumulation.

As a consequence, it appears reasonable to set the focus on the modelling of nonlinear fatigue damage accumulation, which is related to the fatigue damage evolution in Eq. (22.12). The following approach is proposed in Kroll and Matzenmiller (2017):

$$\dot{D}_{\mathrm{f}} = \frac{\left(1-(1-D)^{k+1}\right)^{\alpha}}{1-\alpha} \left( \frac{\langle \sigma_{\mathrm{eqf}} - \sigma_{\mathrm{df}} \rangle}{(\sigma_{\mathrm{u}} - \sigma_{\mathrm{df}})(1-D)} \right)^{k} \frac{\langle \dot{\sigma}_{\mathrm{eqf}} \rangle}{\sigma_{\mathrm{u}} - \sigma_{\mathrm{df}}} \,. \tag{22.33}$$

By contrast with Eq. (22.12), the fatigue damage evolution in Eq. (22.33) has an additional factor, which contains the variable $\alpha$ for nonlinear fatigue damage accumulation. In the following, $\alpha$ is assumed to be a function, which is constant for any integration over a stress cycle, resulting in a damage increment according to Eqs. (22.16), (22.17):

$$\alpha = \alpha(\sigma_{\mathrm{eqfmin}}, \sigma_{\mathrm{eqfmax}}) \,. \tag{22.34}$$

The following approach for $\alpha$ in Kroll and Matzenmiller (2017) is based on the proposals in Chaboche and Lesne (1988) and Do et al (2015):

$$\alpha = \alpha_{\mathrm{p2}} \left( \left\langle 1 - \alpha_{\mathrm{p1}} \left\langle \frac{\sigma_{\mathrm{eqfa}} - \sigma_{\mathrm{df}}}{\tau_{\mathrm{u}} - \sigma_{\mathrm{eqfmax}}} \right\rangle - \alpha_{\mathrm{p3}} \right\rangle + \alpha_{\mathrm{p3}} \right) \,. \tag{22.35}$$

In Eq. (22.35), $\alpha_{\mathrm{p1}}$, $\alpha_{\mathrm{p2}}$ and $\alpha_{\mathrm{p3}}$ are parameters. The first parameter $\alpha_{\mathrm{p1}}$ controls the damage interaction (Chaboche and Lesne, 1988), which is not addressed in this

contribution. The switching variable $\alpha_{\mathrm{p2}}$ is used in order to set $\alpha_{\mathrm{p2}} = 0 \rightarrow \alpha = 0$, which results in linear fatigue damage accumulation, see Subsect. 22.3.3. The third parameter $\alpha_{\mathrm{p3}}$ represents a lower boundary for $\alpha$ for the stabilisation of the numerical treatment (Kroll and Matzenmiller, 2017).

As in Subsect. 22.2.2, three integrations of the damage equation (22.33) will be presented for pure fatigue damage $D = D_{\mathrm{f}}$. Thus, Eq. (22.33) becomes

$$\mathrm{d}D_{\mathrm{f}} = \frac{\left(1-(1-D_{\mathrm{f}})^{k+1}\right)^{\alpha}}{1-\alpha} \left( \frac{\langle \sigma_{\mathrm{eqf}} - \sigma_{\mathrm{df}} \rangle}{(\sigma_{\mathrm{u}} - \sigma_{\mathrm{df}})(1-D_{\mathrm{f}})} \right)^{k} \frac{\langle \mathrm{d}\sigma_{\mathrm{eqf}} \rangle}{\sigma_{\mathrm{u}} - \sigma_{\mathrm{df}}} \,. \tag{22.36}$$

The first solution is obtained by separation and integration until rupture according to Eqs. (22.15) to (22.18) for CA fatigue loading, for which $\alpha$ is constant due to Eq. (22.34):

$$\int_0^1 \frac{(1-\alpha)(1-D_{\mathrm{f}})^k}{\left(1-(1-D_{\mathrm{f}})^{k+1}\right)^{\alpha}} \mathrm{d}D_{\mathrm{f}} = \int_0^{N_{\mathrm{R}}} \int_{\sigma_{\mathrm{eqfmin}}}^{\sigma_{\mathrm{eqfmax}}} \left( \frac{\sigma_{\mathrm{eqf}} - \sigma_{\mathrm{df}}}{\sigma_{\mathrm{u}} - \sigma_{\mathrm{df}}} \right)^{k} \frac{\mathrm{d}\sigma_{\mathrm{eqf}}}{\sigma_{\mathrm{u}} - \sigma_{\mathrm{df}}} \mathrm{d}N, \tag{22.37}$$

$$\frac{1}{k+1} \int_0^1 \frac{1-\alpha}{\tilde{D}^{\alpha}} \mathrm{d}\tilde{D} = \int_0^{N_{\mathrm{R}}} \int_{\sigma_{\mathrm{eqfmin}}}^{\sigma_{\mathrm{eqfmax}}} \left( \frac{\sigma_{\mathrm{eqf}} - \sigma_{\mathrm{df}}}{\sigma_{\mathrm{u}} - \sigma_{\mathrm{df}}} \right)^{k} \frac{\mathrm{d}\sigma_{\mathrm{eqf}}}{\sigma_{\mathrm{u}} - \sigma_{\mathrm{df}}} \mathrm{d}N, \tag{22.38}$$

$$\Rightarrow N_{\mathrm{R}} = \frac{(\sigma_{\mathrm{u}} - \sigma_{\mathrm{df}})^{k+1}}{(\sigma_{\mathrm{eqfmax}} - \sigma_{\mathrm{df}})^{k+1} - (\sigma_{\mathrm{eqfmin}} - \sigma_{\mathrm{df}})^{k+1}} \,, \tag{22.39}$$

where the following substitution has been used:

$$\tilde{D} = 1 - (1-D_{\mathrm{f}})^{k+1} \quad , \quad \mathrm{d}\tilde{D} = (k+1)(1-D_{\mathrm{f}})^{k} \mathrm{d}D_{\mathrm{f}} \,. \tag{22.40}$$

Since the numbers of cycles to rupture in Eqs. (22.19) and (22.39) are equal, the term with $\alpha$ has no influence on the lifetime for CA loading.

According to the limits for integration in Eq. (22.21), the integration of Eq. (22.36) from the virgin state until a certain amount of damage $D$ for CA loading together with the substitution in Eq. (22.40) and constant $\alpha$ due to Eq. (22.34) yields

$$\int_0^D \frac{(1-\alpha)(1-D_{\mathrm{f}})^k}{\left(1-(1-D_{\mathrm{f}})^{k+1}\right)^{\alpha}} \mathrm{d}D_{\mathrm{f}} = \int_0^{N} \int_{\sigma_{\mathrm{eqfmin}}}^{\sigma_{\mathrm{eqfmax}}} \left( \frac{\langle \sigma_{\mathrm{eqf}} - \sigma_{\mathrm{df}} \rangle}{\sigma_{\mathrm{u}} - \sigma_{\mathrm{df}}} \right)^{k} \frac{\mathrm{d}\sigma_{\mathrm{eqf}}}{\sigma_{\mathrm{u}} - \sigma_{\mathrm{df}}} \mathrm{d}\tilde{N}, \tag{22.41}$$

$$D = 1 - \left( 1 - \left( \frac{N}{N_{\mathrm{R}}} \right)^{\frac{1}{1-\alpha}} \right)^{\frac{1}{k+1}} \,. \tag{22.42}$$

As can be seen from the comparison of Eq. (22.42) with Eq. (22.21), in addition to the parameter $k$, the variable $\alpha$ has also an influence on the course of damage over the cycle ratio.

The last integration is performed for a damage increment according to the limits in Eq. (22.22) and by use of the substitution in Eq. (22.40), which results in the following expression for actual damage $D_i$, where $\alpha_i = \alpha_i(\sigma_{\mathrm{eqfmin},i}, \sigma_{\mathrm{eqfmax},i})$ is constant for every load level $i$, cf. Eq. (22.34):

$$\frac{1}{k+1}\int\limits_{\tilde{D}_{i-1}}^{\tilde{D}_i}\frac{1-\alpha_i}{\tilde{D}^{\alpha_i}}\mathrm{d}\tilde{D} = \int\limits_{N_{i-1}}^{N_{i-1}+\Delta N_i}\int\limits_{\sigma_{\mathrm{eqfmin},i}}^{\sigma_{\mathrm{eqfmax},i}}\left(\frac{\sigma_{\mathrm{eqf}}-\sigma_{\mathrm{df}}}{\sigma_{\mathrm{u}}-\sigma_{\mathrm{df}}}\right)^k\frac{\mathrm{d}\sigma_{\mathrm{eqf}}}{\sigma_{\mathrm{u}}-\sigma_{\mathrm{df}}}\mathrm{d}N\ , \tag{22.43}$$

$$D_i = 1-\left(1-\left[\left(1-\left[1-D_{i-1}\right]^{k+1}\right)^{1-\alpha_i}+\frac{\Delta N_i}{N_{\mathrm{R}i}}\right]^{\frac{1}{1-\alpha_i}}\right)^{\frac{1}{k+1}}\ . \tag{22.44}$$

The variable $\alpha_i$ in Eq. (22.44) has an additional influence on the actual amount of damage compared to Eq. (22.23), as observed by comparing of Eqs. (22.42) and (22.21).

### *22.3.3 Discussion of Modelling Approach*

In the following, the damage accumulation behaviour of Eq. (22.36) will be analysed as already performed for Eq. (22.14) in Subsect. 22.3.1. According to Eqs. (22.44) and (22.42), damage due to CA fatigue loading over $\Delta N_1$ loading cycles from the undamaged state to damage $D_i$ with $i = 1$ and $D_0 = 0$ is

$$D_1 = 1-\left(1-\left(\frac{\Delta N_1}{N_{\mathrm{R1}}}\right)^{\frac{1}{1-\alpha_1}}\right)^{\frac{1}{k+1}}\ . \tag{22.45}$$

If further loading with a second load level is applied, according to Eq. (22.44), damage after this second load level then is

$$D_2 = 1-\left(1-\left[\left(1-\left[1-D_1\right]^{k+1}\right)^{1-\alpha_2}+\frac{\Delta N_2}{N_{\mathrm{R2}}}\right]^{\frac{1}{1-\alpha_2}}\right)^{\frac{1}{k+1}}\ . \tag{22.46}$$

Insertion of Eq. (22.45) into Eq. (22.46) results in

$$D_2 = 1-\left(1-\left[\left(\frac{\Delta N_1}{N_{\mathrm{R1}}}\right)^{\frac{1-\alpha_2}{1-\alpha_1}}+\frac{\Delta N_2}{N_{\mathrm{R2}}}\right]^{\frac{1}{1-\alpha_2}}\right)^{\frac{1}{k+1}}\ . \tag{22.47}$$

If the second load level is applied until rupture, then $D_2 = 1$ in Eq. (22.47), becoming

$$\left(\frac{\Delta N_1}{N_{\mathrm{R}1}}\right)^{\frac{1-\alpha_2}{1-\alpha_1}} + \frac{\Delta N_2}{N_{\mathrm{R}2}} = 1. \tag{22.48}$$

If the second and third level do not result in rupture, then insertion of Eq. (22.47) into Eq. (22.44) for $i = 3$ yields the following amount of damage:

$$D_3 = 1 - \left(1 - \left[\left[\left(\frac{\Delta N_1}{N_{\mathrm{R}1}}\right)^{\frac{1-\alpha_2}{1-\alpha_1}} + \frac{\Delta N_2}{N_{\mathrm{R}2}}\right]^{\frac{1-\alpha_3}{1-\alpha_2}} + \frac{\Delta N_3}{N_{\mathrm{R}3}}\right]^{\frac{1}{1-\alpha_3}}\right)^{\frac{1}{k+1}}. \tag{22.49}$$

If rupture occurs after load level $K = 3$, then $D_3 = 1$ and Eq. (22.49) becomes

$$\left[\left(\frac{\Delta N_1}{N_{\mathrm{R}1}}\right)^{\frac{1-\alpha_2}{1-\alpha_1}} + \frac{\Delta N_2}{N_{\mathrm{R}2}}\right]^{\frac{1-\alpha_3}{1-\alpha_2}} + \frac{\Delta N_3}{N_{\mathrm{R}3}} = 1. \tag{22.50}$$

The preceding steps can be performed for a block loading with arbitrary number of load levels. Damage after load level $j$ is

$$D_j = 1 - \left(1 - \left[\left[\ldots\left[\left[\left(\frac{\Delta N_1}{N_{\mathrm{R}1}}\right)^{\frac{1-\alpha_2}{1-\alpha_1}} + \frac{\Delta N_2}{N_{\mathrm{R}2}}\right]^{\frac{1-\alpha_3}{1-\alpha_2}} + \frac{\Delta N_3}{N_{\mathrm{R}3}}\right]^{\frac{1-\alpha_4}{1-\alpha_3}} \ldots + \frac{\Delta N_{j-1}}{N_{\mathrm{R}j-1}}\right]^{\frac{1-\alpha_j}{1-\alpha_{j-1}}} + \frac{\Delta N_j}{N_{\mathrm{R}j}}\right]^{\frac{1}{1-\alpha_j}}\right)^{\frac{1}{k+1}}. \tag{22.51}$$

If rupture occurs after load level $K$, then $D_j = D_K = 1$ in Eq. (22.51), which becomes

$$\left[\ldots\left[\left[\left(\frac{\Delta N_1}{N_{\mathrm{R}1}}\right)^{\frac{1-\alpha_2}{1-\alpha_1}} + \frac{\Delta N_2}{N_{\mathrm{R}2}}\right]^{\frac{1-\alpha_3}{1-\alpha_2}} + \frac{\Delta N_3}{N_{\mathrm{R}3}}\right]^{\frac{1-\alpha_4}{1-\alpha_3}} \ldots + \frac{\Delta N_{K-1}}{N_{\mathrm{R}K-1}}\right]^{\frac{1-\alpha_K}{1-\alpha_{K-1}}} + \frac{\Delta N_K}{N_{\mathrm{R}K}} = 1. \tag{22.52}$$

The difference of Eq. (22.52) compared to the PALMGREN–MINER rule in Eq. (22.25) is, that the cycle ratios are not commutatively superimposed, which is nonlinearity of damage accumulation in the sense of noncommutativity of the chronological order of the load levels.

This property becomes apparent, if the PALMGREN–MINER rule in Eq. (22.25) is interpreted as a chain formed by the cycle ratios as summands, then the chain links can be arbitrarily interchanged without any change of the result. In the simplest case of two load levels until rupture, this means commutativity of $\Delta N_1/N_{\mathrm{R}1} + \Delta N_2/N_{\mathrm{R}2} = \Delta N_2/N_{\mathrm{R}2} + \Delta N_1/N_{\mathrm{R}1} = 1$. In the case of Eq. (22.52), the chain links cannot be interchanged without any change of the result. Consider for example

the particular case of $K = 2$ load levels in Eq. (22.48), which is equivalent to

$$\frac{\Delta N_1}{N_{\mathrm{R1}}} = \left(1 - \frac{\Delta N_2}{N_{\mathrm{R2}}}\right)^{\frac{1-\alpha_1}{1-\alpha_2}}, \tag{22.53}$$

where the loading $\sigma_{\mathrm{eqf},1}$ with $\sigma_{\mathrm{eqfmin},1}$ and $\sigma_{\mathrm{eqfmax},1}$ of level one is applied first, followed by the loading $\sigma_{\mathrm{eqf},2}$ with $\sigma_{\mathrm{eqfmin},2}$ and $\sigma_{\mathrm{eqfmax},2}$ of level two until rupture. If the chronological order of the load levels is interchanged, then the result is different from Eq. (22.53):

$$\left(\frac{\Delta N_2}{N_{\mathrm{R2}}}\right)^{\frac{1-\alpha_1}{1-\alpha_2}} + \frac{\Delta N_1}{N_{\mathrm{R1}}} = 1 \Leftrightarrow \frac{\Delta N_1}{N_{\mathrm{R1}}} = 1 - \left(\frac{\Delta N_2}{N_{\mathrm{R2}}}\right)^{\frac{1-\alpha_1}{1-\alpha_2}}. \tag{22.54}$$

The same observation holds for the general case with $K$-level loading in Eq. (22.52), which, therefore, considers the loading sequence effect. Linear damage accumulation results from the case $\alpha_i = \alpha_j$ for all $i, j$ or particularly $\alpha = 0$, then Eq. (22.52) becomes the PALMGREN–MINER rule in Eq. (22.25).

Although nonlinear damage accumulation can be further investigated by means of the general case in Eq. (22.52), the particular case $K = 2$ is much simpler, represented by Eqs. (22.53) and (22.54). If $\alpha_{\mathrm{p2}} = 1$ and

$$1 - \alpha_{\mathrm{p1}} \left\langle (\sigma_{\mathrm{eqfa}} - \sigma_{\mathrm{df}})/(\tau_{\mathrm{u}} - \sigma_{\mathrm{eqfmax}}) \right\rangle > \alpha_{\mathrm{p3}},$$

then the insertion of the approach for $\alpha$ given by Eq. (22.35) into Eqs. (22.53) and (22.54) results in the following expressions, which are independent of the parameter $\alpha_{\mathrm{p1}}$ due to the division in the exponent:

$$\frac{\Delta N_1}{N_{\mathrm{R1}}} = \left(1 - \frac{\Delta N_2}{N_{\mathrm{R2}}}\right)^{\frac{\left\langle (\sigma_{\mathrm{eqfa},1} - \sigma_{\mathrm{df}})/(\tau_{\mathrm{u}} - \sigma_{\mathrm{eqfmax},1}) \right\rangle}{\left\langle (\sigma_{\mathrm{eqfa},2} - \sigma_{\mathrm{df}})/(\tau_{\mathrm{u}} - \sigma_{\mathrm{eqfmax},2}) \right\rangle}}, \tag{22.55}$$

$$\frac{\Delta N_1}{N_{\mathrm{R1}}} = 1 - \left(\frac{\Delta N_2}{N_{\mathrm{R2}}}\right)^{\frac{\left\langle (\sigma_{\mathrm{eqfa},1} - \sigma_{\mathrm{df}})/(\tau_{\mathrm{u}} - \sigma_{\mathrm{eqfmax},1}) \right\rangle}{\left\langle (\sigma_{\mathrm{eqfa},2} - \sigma_{\mathrm{df}})/(\tau_{\mathrm{u}} - \sigma_{\mathrm{eqfmax},2}) \right\rangle}}. \tag{22.56}$$

The same observation is made for the damage accumulation by Eq. (22.52). Hence, in the case of pure fatigue, the parameter $\alpha_{\mathrm{p1}}$ in Eq. (22.35) does not influence the damage accumulation behaviour, but only influences the course of damage over the cycle ratio for one-level loading until rupture, which becomes apparent by insertion of Eq. (22.35) into Eq. (22.42).

## 22.4 Parameter Identification

Creep loading is the special case of CA loading, where the global extrema coincide. Thus, the parameter identification starts with the direct determination of

the creep damage parameters $\sigma_{\mathrm{dc}}$, $\sigma_{\mathrm{ref}}$ and $n$ by means of creep tests until rupture as illustrated in Fig. 22.1(a), where pure shear is considered: $t_{\mathrm{n}} = t_{\mathrm{b}} = 0$, $\sigma_{\mathrm{eqc}} = \sigma_{\mathrm{eqf}} = t_{\mathrm{t}}$. Afterwards, the fatigue damage parameters $\sigma_{\mathrm{df}}$, $\sigma_{\mathrm{u}}$ and $k$ are identified directly by means of tests with CA pure shear fatigue loading as shown in Fig. 22.1(b). Since the illustration in Fig. 22.1(b) is only true for negligible creep damage, the fatigue damage parameters $\sigma_{\mathrm{u}}$ and $k$ need to be numerically optimised. However, as mentioned in Subsect. 22.3.2, creep damage is expected to be negligible for usual HCF loading and the values of the identified parameters are expected to be marginally changed by the optimisation. After the determination of the damage model parameters by means of creep and CA fatigue tests with pure shear, the shear-tension interaction parameters $b_{1\mathrm{c}}$, $b_{2\mathrm{c}}$, $b_{1\mathrm{f}}$ and $b_{2\mathrm{f}}$ are directly identified and numerically optimised by means of multiaxial creep and CA fatigue tests. The validity of the parameter identification has been shown in Kroll and Matzenmiller (2015, 2016, 2017) and Kroll (2018).

As pointed out in Subsect. 22.3.2, the modelling approach for nonlinear fatigue damage accumulation has no influence on the lifetime prediction for CA loading in the case of pure fatigue, see Eq. (22.39). Thus, material dependent parameters in the approach for the function $\alpha = \alpha(\sigma_{\mathrm{eqfmin}}, \sigma_{\mathrm{eqfmax}})$ in Eq. (22.34) may be determined by means of one of the following two sets of test data: The first set contains the results of two-level loading tests, for which the parameters in the function $\alpha$ have to be determined in order to fit Eqs. (22.53) and (22.54) with the test data. Thereby, the parameters to be identified must have an influence on the rupture time, contrary to parameter $\alpha_1$ in the approach for $\alpha$ in Eq. (22.35), see Eqs. (22.55) and (22.56). An alternative way for the identification procedure is the evaluation of the damage values over the cycle ratio as the second set of test data. In this case, the parameters in $\alpha$ have to be identified in order to fit Eq. (22.42) with the data points. Unfortunately, damage is an internal variable and cannot be measured directly, but only indirectly by means of several methods, see Lemaitre and Dufailly (1987). The main difficulties are the reasonable choice and the reliable detection of the quantity, which is supposed to represent damage best for the particular case of application.

For the previous explained direct identification of the parameters in $\alpha$, creep damage must be negligible compared to fatigue damage, which is the necessary condition for the application of the Eqs. (22.36) to (22.54). If this is not the case, then the fatigue damage parameters $\sigma_{\mathrm{u}}$, $\sigma_{\mathrm{df}}$ and $k$ as well as the parameters in the function $\alpha$ have to be numerically and simultaneously optimised in a last step by means of S-N curves and rupture times from two-level loadings or indirect damage measurements.

The tests for the parameter identification must provide an almost homogeneous state of stress in the bonding layer. Therefore, the adhesive layer thickness must be very thin in order to describe its constitutive behaviour by a cohesive zone model, see e.g. Su et al (2004). This applies to structural adhesives, which usually have a bonding layer thickness between 0.1 and 1 mm. Second, the geometries of the adherends as well as the load application in the test setup must be appropriate such that peeling and inhomogeneous shear loading is minimised. Examples are the specimens with single lap and butt joints and the corresponding test setups in Schlim-

mer et al (2012); Schneider et al (2012) and Cavdar and Meschut (2017) providing almost homogeneous shear-, tension- and combined shear and tension in the thin structural adhesive bonding layer.

## 22.5 Application to Lifetime Prediction for Adhesive Joints

In the following, the application in Kroll and Matzenmiller (2017) and Kroll (2018) of the proposed damage model is presented for the lifetime prediction of butt-bonded thin steel tubes under two-level torsional loading with force control until rupture. The bonding layer consists of the thermosetting, one-component, ductile modified epoxy structural adhesive BETAMATE™1496V and has a thickness of $0.3$ mm only. Therefore, it is modelled as a cohesive zone, which suffers pure shear stress $t_{\mathrm{t}}$ due to the torsional loading of the specimen. The preparation of the adherends, the bonding procedure and the test setup are detailly described in Cavdar and Meschut (2017).

The test results in Fig. 22.3 show nonlinear damage accumulation due to LH loading, while the data points for HL loading almost coincide with the dashed line, representing linear damage accumulation. The location of some data points outside the unit square may be explained by the scatter of the data, because this phenomenon exists for both the LH and HL sequence. Another explanation refers to an effect of the firstly applied load level, which in some situations, mostly for LH loading, increases the fatigue life for the subsequently applied load level. For an amount of loading cycles below $\Delta N_2 = 0.5 N_{\mathrm{R2}}$, this effect may even increase the original CA fatigue life.

Since the model equations in this contribution do not account for scatter of data and the previously mentioned effect of lifetime increase, only the unit square is il-

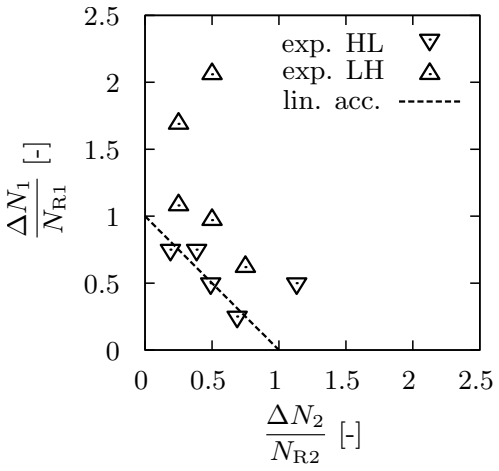


**Fig. 22.3** Experimental test data (Cavdar and Meschut, 2017) due to High-Low (HL) and Low-High (LH) two-level shear loading with $f = 10$ Hz; number of cycles to rupture for high loading (in MPa) $t_{\mathrm{t1}} = 16.97 + 13.88 \sin(2\pi f t)$ is $N_{\mathrm{R1}} = 5663$ and for low loading (in MPa) $t_{\mathrm{t2}} = 13.2 + 10.8 \sin(2\pi f t)$ is $N_{\mathrm{R2}} = 713246$

lustrated in Fig. 22.4, where lifetime predictions are compared with the test results. The predictions denoted with ODE1, ODE2 and ODE3 result from the implicit nu-

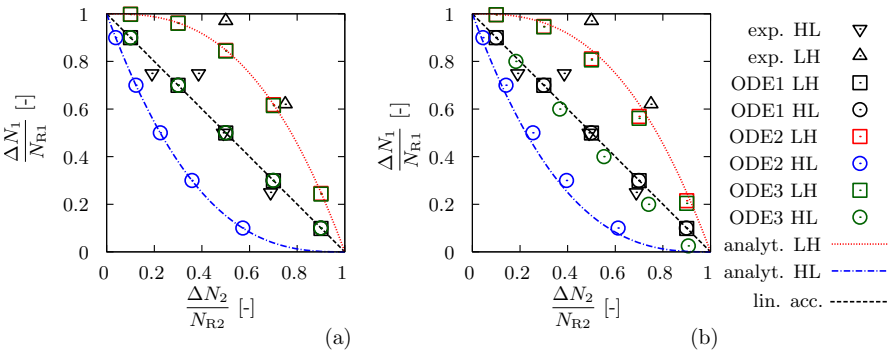


**Fig. 22.4** Experimental test data and prediction for two-level loading in Fig. 22.3 for (a) pure fatigue ($\dot{D}_c = 0$) and (b) creep-fatigue; ODE1: Eqs. (22.3), (22.4), (22.5), (22.12), (22.13); ODE2: Eqs. (22.3), (22.4), (22.5), (22.13) (22.33), (22.35); ODE3: Eqs. (22.3), (22.4), (22.5), (22.13), (22.35), (22.57), (22.58); analyt. HL: Eq. (22.55); analyt. LH: Eq. (22.56)

merical solution of the corresponding damage evolution equation, for which the two step backward differentiation formula together with the second order finite difference approximation are applied, see Kroll and Matzenmiller (2015). Besides the presented model equations in the previous sections, the following expressions are additionally considered for ODE3:

$$\dot{D}_f = \frac{\left(1-(1-D)^{k+1}\right)^{\alpha_{min}}}{1-\alpha_{min}} \left( \frac{\langle \sigma_{eqf} - \sigma_{df} \rangle}{(\sigma_u - \sigma_{df})(1-D)} \right)^k \frac{\langle \dot{\sigma}_{eqf} \rangle}{\sigma_u - \sigma_{df}}, \tag{22.57}$$

$$\alpha_{min}(t) = \min_{0 \le \tau \le t} \alpha(\tau) \, . \tag{22.58}$$

The damage model parameters in Tabelle 22.1 are identified and optimised according to Kroll and Matzenmiller (2017); Kroll (2018) as explained in Sect. 22.4 by means of data from tests of the steel tube specimen under torsional creep and CA fatigue loading, see Cavdar and Meschut (2017). The parameters in the equivalent stresses given by Eqs. (22.5) and (22.13) are irrelevant in the following due to pure shear loading. The factor for nonlinear damage accumulation is active for all numer-

**Table 22.1** Identified damage model parameters in Kroll and Matzenmiller (2017); Kroll (2018) by means of test data in Cavdar and Meschut (2017)

| $\sigma_{dc}$ [MPa] | $\sigma_{ref}$ [MPa] | $n$ [-] | $\sigma_{df}$ [MPa] | $\sigma_u$ [MPa] | $k$ [-] | $\alpha_{p1}$ [-] | $\alpha_{p2}$ [-] | $\alpha_{p3}$ [-] | $\tau_u$ [MPa] |
|---|---|---|---|---|---|---|---|---|---|
| 0 | 51 | 19 | 0 | 49 | 19 | 1 | 1 | -10 | 39 |

ical computations: $\alpha_{\mathrm{p2}} = 1$. Since no data for the course of damage over cycles or time are considered, the identification of parameter $\alpha_{\mathrm{p1}}$ is obsolete, thus: $\alpha_{\mathrm{p1}} = 1$. The parameter $\alpha_{\mathrm{p3}} = -10$ in Eq. (22.35) is applied for numerical stability, see Kroll and Matzenmiller (2017) and Kroll (2018) for details. The ultimate shear strength $\tau_{\mathrm{u}} = 39$ MPa is identified by means of torsion tests of the steel tube specimen under quasistatic loading Cavdar and Meschut (2017).

The amplitude and maximum of $\sigma_{\mathrm{eqf}}$ in Eq. (22.35) are computed from stress values in the last half cycle, which consists of the most recently passed local minimum and maximum stress as well as the values in between. A detailed description and an alternative formulation are given in Kroll and Matzenmiller (2017); Kroll (2018).

Due to the consideration of pure fatigue damage in Fig. 22.4(a), the numerical predictions for ODE1, ODE2 and ODE3 match with the analytical expressions in the previous sections. Since ODE1 becomes a separable differential equation for pure fatigue damage, it represents linear damage accumulation and the predictions match with the dashed black line, represented by Eq. (22.32) for $K = 2$. The predictions with ODE2 match with Eqs. (22.55) and (22.56), which verifies the numerical solution. The predictions with ODE2 are in better agreement with the test data compared to ODE1 for the LH sequence. But they are worse for the HL sequence. As ODE3 matches with the dotted red line and with the black dashed line, it provides the best results for the representation of the damage accumulation of the structural adhesive at hand. Thereby, Eq. (22.58) ensures $\alpha$ to be constant for the HL scenario in order to match the prediction with the dashed black line for linear accumulation, since $\alpha_1 = -1.252$ and $\alpha_2 = 0.169$, cf. Fig. 22.3.

In Fig. 22.4(b), ODE1 represents nonlinear damage accumulation again because of $n = k$, which is a result of the identification for creep and CA fatigue loading, see Table 22.1. The predictions with ODE2 differ from the curves represented by Eqs. (22.55) and (22.56), which shows the influence of creep damage. The predictions with ODE3 are still in best agreement with the test data.

## 22.6 Conclusion

In this contribution, nonlinear damage accumulation is modelled by a damage differential equation with a creep and fatigue part for the consideration of the loading sequence effect. Three integrations of the differential equation are presented for one-level loading, where different integration limits are applied in order to get three results: the time to rupture and the course of damage over time, both for the initially undamaged state, as well as the damage increment due to a load level. These three results are used to demonstrate the damage accumulation behaviour for pure creep and fatigue damage. They represent the Robinson and Palmgren–Miner rules of linear damage accumulation, if the underlying damage differential equation is separable and confirm that nonlinear damage evolution not automatically implies nonlinear damage accumulation.

The magnitude of creep damage is low compared to fatigue damage for usual HCF loading, which justifies the consideration of pure fatigue damage for the modelling of nonlinear damage accumulation. An adaption is proposed of the fatigue damage part by a factor, which contains the approach for variable $\alpha$ and influences the course of damage over time and the lifetime prediction due to VA loading, but not the prediction due to CA loading. The definition of the variable $\alpha$ ensures separability of the damage equation for each load level in the case of pure fatigue damage, but inseparability in general. Thus, nonlinear damage accumulation can be modelled independently from the S-N approach for CA loading. This is shown by the three integrations of the damage differential equation with different limits, providing a procedure for the identification of the parameters in the function for $\alpha$.

Two particular approaches for $\alpha$ are validated by means of the comparison of numerical lifetime predictions with test data for an adhesive layer subjected to shear loading. Since the predictions are in good agreement with the test data, it is concluded that the loading sequence effect is well captured for pure shear loading.

Nonlinear creep damage accumulation is not considered, but it can be modelled similarly to the fatigue damage accumulation (Kroll, 2018). Although the influences of mean stress, pressure, multiaxiality and nonproportionality on the lifetime for CA loading and the corresponding considerations by the damage model are addressed in Kroll and Matzenmiller (2015, 2017) and Kroll (2018), they have to be experimentally investigated for VA loading of structural adhesives in order to further validate the proposed approach for the variable $\alpha$ according to the presented theory. Therefore, multiaxial tests with two-level loading and different mean stresses as well as indirect damage measurement for one-level loading have to be performed.

## References

Basquin OH (1910) The exponential law of endurance tests. ASTM 10:625–630

Cailletaud G, Levaillant C (1984) Creep-fatigue life prediction: what about initiation? Nucl Eng Des 84:279–292

Cailletaud G, Nouailhas D, Grattier J, Levaillant C, Mottot M, Tortel J, Escavarage C, Héliot J, Kang S (1984) A review of creep-fatigue life prediction methods: identification and extrapolation to long term and low strain cyclic loading. Nucl Eng Des 83:267–278

Cavdar S, Meschut G (2017) Analyse der Schwingfestigkeit geklebter Stahlverbindungen unter mehrkanaliger Belastung. Tech. rep., Forschungsvereinigung Stahlanwendung e.V., number = FOSTA-Report P1028, chap 11-12, Düsseldorf

Cavdar S, Kroll U, Meschut G, Matzenmiller A (2018) Experimental characterization and numerical lifetime prediction of adhesively bonded joints under multiaxial fatigue loading. In: Proc Adh Soc 2018

Chaboche JL (1978) Description thermodynamique et phénoménologique de la viscoplasticité cyclique avec endommagement. Dissertation, Université Pierre et Marie Curie, Paris

Chaboche JL (1981) Continuous damage mechanics — A tool to describe phenomena before crack initiation. Nucl Eng Des 64(2):233–247

Chaboche JL (1987) Continuum damage mechanics: present state and future trends. Nucl Eng Des 105:19–33

Chaboche JL (1988a) Continuum damage mechanics: Part I - general concepts. J Appl Mech 55:59–64
Chaboche JL (1988b) Continuum damage mechanics: Part II - damage growth, crack initiation, and crack growth. J Appl Mech 55:65–72
Chaboche JL (2003) Damage Mechanics. In: Karihaloo B, Knauss WG (eds) Fundamental Theories and Mechanisms of Failure, Elsevier, Comprehensive Structural Integrity, vol 2, pp 213–284
Chaboche JL (2011) Cumulative Damage. In: Bathias C, Pineau A (eds) Fatigue of Materials and Structures, John Wiley & Sons
Chaboche JL, Lesne PM (1988) A non-linear continous fatigue damage model. Fatigue Fract Eng Mater Struct 11(1):1–17
Coleman BD, Gurtin ME (1967) Thermodynamics with internal state variables. J Chem Phys 47(2):597–613
Do VNV, Lee CH, Chang KH (2015) High cycle fatigue analysis in presence of residual stresses by using a continuum damage mechanics model. Int J Fatigue 70:51–62
Erpolat S, Ashcroft IA, Crocombe AD, Abdel-Wahab MM (2004) A study of adhesively bonded joints subjected to constant and variable amplitude fatigue. Int J Fatigue 26(11):1189–1196
Kachanov LM (1958) On rupture time under conditions of creep. Izv Akad Nauk Sssr Otdelenie, Otd Tech 8(2631):26–31, in Russian. English translation (1999) Rupture time under creep conditions. Int J Fract 97:11–18.
Krajcinovic D, Lemaitre J (1987) Continuum Damage Mechanics: Theory and Applications. Springer
Kroll U (2018) Modellierung der Schädigungsentwicklung und Lebensdauerprognose für Stahlklebverbindungen unter hochzyklischer Ermüdungsbelastung. Dissertation, Fachbereich Maschinenbau, Universität Kassel
Kroll U, Matzenmiller A (2015) Parameter identification of a damage model for the lifetime prediction of adhesively bonded joints. In: Saanouni K (ed) Damage Mechanics: Theory, Computation and Practice, Trans Tech Publications, Appl Mech Mater, vol 784, pp 300–307
Kroll U, Matzenmiller A (2016) On nonlinear damage accumulation and creep-fatigue interaction of a damage model for the lifetime prediction of adhesively bonded joints. PAMM 16(1):151–152
Kroll U, Matzenmiller A (2017) Analyse der Schwingfestigkeit geklebter Stahlverbindungen unter mehrkanaliger Belastung. Tech. Rep. FOSTA-Report P1028, chap 13-15, Forschungsvereinigung Stahlanwendung e.V., Düsseldorf
Lemaitre J (1979) Damage Modeling for Prediction of Plastic or Creep Fatigue Failure in Structures. In: Proc IASMiRT 1979 (Trans. 5th Intl. Conf. Struct. Mech. React. Tech.)
Lemaitre J (1984) How to use damage mechanics. Nucl Eng Des 80:233–245
Lemaitre J (1996) A Course on Damage Mechanics. Springer
Lemaitre J, Chaboche JL (1975) A Non-Linear Model of Creep-Fatigue Damage Cumulation and Interaction. In: Hult J (ed) Mechanics of Visco-Elastic Media and Bodies, Springer, pp 291–301
Lemaitre J, Chaboche JL (1990) Mechanics of Solid Materials. Cambridge University Press
Lemaitre J, Desmorat R (2005) Engineering Damage Mechanics. Springer
Lemaitre J, Doghri I (1994) Damage 90: a post processor for crack initiation. Comput Methods Appl Mech Eng 115(3–4):197–232
Lemaitre J, Dufailly J (1987) Damage measurements. Eng Fract Mech 28(5–6):643–661
Lemaitre J, Plumtree A (1979) Application of damage concepts to predict creep-fatigue failures. J Eng Mater Technol 101(3):284–292
Matzenmiller A, Kurnatowski B (2012) Schwingfestigkeitsauslegung von geklebten Stahlbauteilen des Fahrzeugbaus unter Belastung mit variablen Amplituden. Tech. Rep. FOSTA-Report P796, pp. 51–101, 133–138, 210–215, Forschungsvereinigung Stahlanwendung e.V., Verlag und Vertriebsgesellschaft mbH, Düsseldorf
Miner MA (1945) Cumulative damage in fatigue. J Appl Mech 67:A159–A164
Murakami S, Ohno N (1981) A Continuum Theory of Creep and Creep Damage. In: Ponter ARS, Hayhurst DR (eds) Creep in Structures, Springer, pp 422–444

Normenausschuss Bauwesen (NABau) im DIN (2010) Eurocode 3: Bemessung und Konstruktion von Stahlbauten - Teil 1-8: Bemessung von Anschlüssen. DIN Deutsches Institut für Normung e. V.

Normenausschuss Bauwesen (NABau) im DIN (2011) Eurocode 9: Bemessung und Konstruktion von Aluminiumtragwerken - Teil 1-3: Ermüdungsbeanspruchte Tragwerke. DIN Deutsches Institut für Normung e. V.

Ostergren WJ, Krempl E (1979) A uniaxial damage accumulation law for time-varying loading including creep-fatigue interaction. J Press Vessel Technol 101:118–124

Paas M, Schreurs P, Brekelmans W (1993) A continuum approach to brittle and fatigue damage: theory and numerical procedures. Int J Solids Struct 30(4):579–599

Palmgren A (1924) Die Lebensdauer von Kugellagern. Zeitschrift des Vereines Deutscher Ingenieure (VDI Zeitschrift) 68(14):339–341

Pavlou D (2001) Creep life prediction under stepwise constant uniaxial stress and temperature conditions. Eng Struct 23(6):656–662

Rabotnov YN (1963) On the Equation of State of Creep. Proc IMechE 1963 (Joint Intl Conf Creep) 178(68):2–117–2–122

Rabotnov YN (1969) Creep rupture. In: Hetenyi M, Vincenti M (eds) Applied Mechanics – Proceedings of the XII International Congress on Applied Mechanics, Springer, pp 342–349

Rennert R, Kullig E, Vormwald M, Esderts A, Siegele D (2012) Rechnerischer Festigkeitsnachweis für Maschinenbauteile aus Stahl, Eisenguss und Aluminiumwerkstoffen: FKM-Richtlinie, 6th edn. Forschungskuratorium Maschinenbau e. V. (FKM), VDMA Verlag

Robinson E (1938) Effect of temperature variation on the creep strength of steels. Trans ASME 160:253–259

Schlimmer M, Hahn O, Hennemann OD, Mihm KM, Jendrny J, Teutenberg D, Brede M, Nagel C (2012) Methodenentwicklung zur Berechnung und Auslegung geklebter Stahlbauteile im Fahrzeugbau bei schwingender Beanspruchung. Tech. Rep. FOSTA-Report P653, Forschungsvereinigung Stahlanwendung e.V., Düsseldorf

Schneider B, Kehlenbeck H, Nagel C (2012) Schwingfestigkeitsauslegung von geklebten Stahlbauteilen des Fahrzeugbaus unter Belastung mit variablen Amplituden. Tech. Rep. FOSTA-Report P796, chap 2, Forschungsvereinigung Stahlanwendung e.V., Düsseldorf

Su C, Wei YJ, Anand L (2004) An elastic–plastic interface constitutive model: application to adhesive joints. Int J Plast 20(12):2063–2081

Todinov M (2001) Necessary and sufficient condition for additivity in the sense of the Palmgren–Miner rule. Comput Mater Sci 21(1):101–110

Truesdell C, Toupin RA (1960) The Classical Field Theories. In: Flügge S (ed) Principles of Classical Mechanics and Field Theory, Handbuch der Physik, vol 3/I, Springer